Cancer Cell
Article

A Conditional Mouse Model of Synovial Sarcoma: Insights into a Myogenic Origin

Malay Haldar,[1] Jeffrey D. Hancock,[2,3] Cheryl M. Coffin,[4] Stephen L. Lessnick,[2,3,5] and Mario R. Capecchi[1,6,*]
[1] Department of Human Genetics
[2] The Division of Pediatric Hematology/Oncology
[3] The Center for Children, Huntsman Cancer Institute
[4] Department of Pathology
[5] Department of Oncological Sciences, Huntsman Cancer Institute
[6] Howard Hughes Medical Institute
University of Utah School of Medicine, Salt Lake City, UT 84112, USA
*Correspondence: mario.capecchi@genetics.utah.edu
DOI 10.1016/j.ccr.2007.01.016

SUMMARY

Synovial sarcoma is an aggressive soft-tissue malignancy marked by a unique t(X;18) translocation leading to expression of a chimeric SYT-SSX fusion protein. We report here a mouse model of synovial sarcoma based on conditional expression of the human SYT-SSX2. Using this model, we have identified myoblasts as a potential source of synovial sarcoma. Remarkably, within the skeletal muscle lineage, while expression of the oncoprotein in immature myoblasts leads to induction of synovial sarcoma with 100% penetrance, its expression in more differentiated cells induces myopathy without tumor induction. We also show that early widespread expression of the fusion protein disrupts normal embryogenesis, causing lethality.

INTRODUCTION

Synovial sarcoma accounts for 7%–10% of all soft-tissue sarcomas, frequently affecting adolescents and young adults. Metastasis is common and usually targeted to lungs, lymph nodes, and bone marrow (Weiss and Goldblum, 2001). The name "synovial sarcoma" was initially coined for tumors arising near joints and having some microscopic resemblance to synovial tissue. However, this tumor can arise, although rarely, in sites away from joints such as head and neck, pharynx, lungs, and heart, which contradicts this nomenclature. Several studies have demonstrated a lack of synovial differentiation in synovial sarcoma tumor cells and showed that these tumors express markers of both epithelial and mesenchymal differentiation, although they do not resemble any specific tissue type (Fisher, 1986; Smith et al., 1995). Synovial sarcoma is now regarded as a neoplasm of "uncertain differentiation." Based on histopathology, synovial sarcomas are divided into biphasic, monophasic, and poorly differentiated subtypes. The presence of epithelioid cells often arranged in whorls or primitive gland-like structures along with the presence of spindle-shaped cells is a hallmark of the biphasic subtype, while the monophasic subtype is marked by a predominance of spindle cells. The poorly differentiated subtype comprises primitive small round cells similar to Ewing's sarcoma. Immunohistochemistry plays an important role in diagnosis, the hallmark being expression of both epithelial markers (cytokeratins) and mesenchymal markers (vimentin). *Bcl-2* overexpression is also frequently observed in these tumors (Hibshoosh and Lattes, 1997; Pelmus et al., 2002).

Synovial sarcoma is marked by a signature genetic event, the t(X;18) translocation-mediated fusion of the *SYT* gene on chromosome 18q11 to either *SSX1*, *SSX2*, or, very rarely, the *SSX4* gene located on chromosome

SIGNIFICANCE

Synovial sarcoma is an aggressive, malignant soft-tissue tumor associated with significant mortality and morbidity. The origin and pathogenesis of this disease are poorly understood, and response to current therapeutic modalities is unsatisfactory. We report here a mouse model of synovial sarcoma that should significantly aid our efforts to understand the pathogenesis of this disease and provide us with a reliable preclinical platform to design and evaluate therapeutic strategies. The identification of a potential cell of origin for this disease and other interesting observations with this model highlight its value and underscores the utility of the conditional genetic approach in cancer modeling.

Xp11 (Clark et al., 1994; Crew et al., 1995; de Leeuw et al., 1995; dos Santos et al., 2001; Limon et al., 1986; Panagopoulos et al., 2001; Skytting et al., 1999; Smith et al., 1987). This translocation is specific to synovial sarcoma. While the presence of SYT-SSX transcript is considered diagnostic for synovial sarcoma, the reciprocal *SSX-SYT* transcripts are frequently absent within these tumors, implicating SYT-SSX as the main suspect in the etiology (Guillou et al., 2001; Hiraga et al., 1998; Ladanyi and Bridge, 2000; Panagopoulos et al., 2001; Poteat et al., 1995; Willeke et al., 1998). Further supporting this notion, studies have demonstrated that human SYT-SSX1 transforms rat fibroblasts, and the transformed cells formed tumors within nude mice (Nagai et al., 2001). The 5′ translocation partner *SYT* is evolutionarily conserved, possesses promoter architecture of housekeeping genes, and is widely expressed in humans and mice (de Bruijn et al., 1996, 2001). It is a putative transcriptional coactivator and is thought to exert its effect by binding to chromatin remodelers (Perani et al., 2003; Thaete et al., 1999). The 3′ translocation partner *SSX* is a family of closely related genes on the X chromosome and is believed to be transcriptional corepressors. SSX expression in adults is restricted to testes, although it is occasionally expressed in certain tumors as well (Clark et al., 1994; Crew et al., 1995; Gure et al., 1997; Lim et al., 1998). The t(X;18)-generated SYT-SSX fusion protein retains the activation domain of SYT along with the repressor domain of SSX, lacks a DNA binding domain, and probably acts via interaction with chromatin remodelers (dos Santos et al., 2000, 2001; Nagai et al., 2001). Several studies have also shown that the type of translocation has a bearing on the prognosis and histology of synovial sarcoma. The *SYT-SSX1* fusion type has been shown to be associated with biphasic histology and a worse prognosis compared to the predominantly monophasic SYT-SSX2 subtype (de Leeuw et al., 1994; Kawai et al., 1998; Ladanyi et al., 2002; Renwick et al., 1995). The underlying molecular basis of these correlations is unknown.

Taking into consideration that synovial sarcoma is a somatic genetic disease and tumorigenesis is dependent upon a permissive microenvironment, we have developed a mouse that conditionally expresses human SYT-SSX2 fusion protein in the presence of site-specific Cre recombinase, thereby allowing us to investigate the transforming role of this protein in chosen tissues at specific times. The tissue or cell of origin for synovial sarcoma is unknown. However, its frequent occurrence within or in proximity to skeletal muscles raises the possibility that transformation of an undifferentiated cell of skeletal muscle lineage gives rise to these tumors. This led us to investigate the skeletal muscle lineage as a potential source of synovial sarcoma. In this study, we report the generation of synovial-sarcoma-like tumors with 100% penetrance in mice expressing SYT-SSX2 within skeletal-muscle-specific *Myf5* lineage. These tumors recapitulate the histopathological, immunohistochemical, and transcriptional profile of human synovial sarcoma.

RESULTS

Generation of Targeted Mouse Lines

Human *SYT-SSX2* cDNA generated from RNA isolated from a synovial sarcoma tumor sample was used to construct conditional SYT-SSX2 targeting vectors for targeting into the mouse *ROSA26* locus on chromosome 6 following published procedures (Srinivas et al., 2001). The *ROSA* promoter is ubiquitously active, thereby allowing transcription of the fusion protein in any chosen tissue following Cre-dependent recombination (Soriano, 1999; Zambrowicz et al., 1997). Two variations of the targeting vector were designed and used to generate two mouse lines, SSM1 (synovial sarcoma mouse 1) and SSM2 (synovial sarcoma mouse 2). SSM2 mice express SYT-SSX2-IRES-EGFP bicistronic mRNA from the endogenous *ROSA* promoter that enables monitoring of SYT-SSX2 expression by detecting EGFP-mediated fluorescence (Figure 1A). The SSM1-targeting construct is similar but lacks the *IRES-EGFP* marker gene. Between the *ROSA26* promoter and the *SYT-SSX2 cDNA* is a strong transcriptional termination signal, *NeoPA*, flanked by *loxP* sites (Figure 1A). In the absence of Cre, *SYT-SSX2* is not transcribed. In the presence of Cre, *Neo-pA* is excised and *SYT-SSX2* transcription commences. By controlling where and when Cre protein is produced, we control where and when SYT-SSX2 fusion protein is made. In the absence of Cre, both homozygous and heterozygous SSM1 and SSM2 mice (SSM denoting either mouse lines) are normal, viable, and fertile with no expression of SYT-SSX2 or EGFP (data not shown).

To induce Cre expression within committed myoblasts expressing the myogenic regulatory factor *Myf5*, we generated a *Myf5-Cre* driver such that Cre is expressed as a second cistron from an *IRES* placed within the 3′UTR of the *Myf5* gene as shown in Figure 1B (Jackson et al., 1990; Jang and Wimmer, 1990). Homozygous and heterozygous *Myf5-Cre* mice are viable and fertile. To confirm the correct expression domain of Cre recombinase in *Myf5-Cre* mice, we bred them to *ROSA-YFP* reporter mice that express the yellow fluorescent protein (YFP) within any Cre-expressing cell and its lineage (Srinivas et al., 2001). *Myf5* is a myogenic regulatory factor that has an important role in the specification of skeletal muscle lineage. Its expression begins early in embryogenesis within immature myoblasts that eventually give rise to adult skeletal muscle (Chanoine et al., 2004; Pownall et al., 2002). Therefore, while early-stage *Myf5-Cre/ROSA-YFP* embryos should have YFP expression within dermomyotome component of somites, later-stage embryos and adults should have YFP expression within skeletal muscle. This was consistently observed in our *Myf5* lineage experiments (Figures 2Aa–2Ad).

SYT-SSX2 Expression within *Myf5* Lineage Induces Tumors

To express SYT-SSX2 within committed myoblasts and their lineage, the conditional SSM (SSM1 or SSM2) mice were bred to *Myf5-Cre* mice, and the resulting

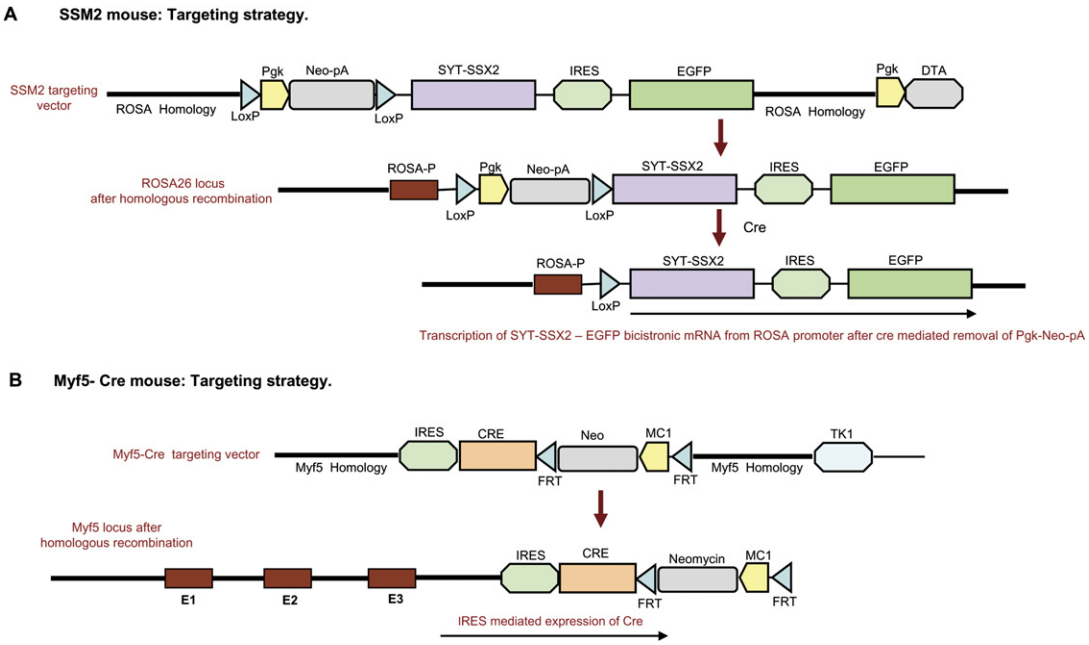

Figure 1. Generation of Targeted Mouse Lines

(A) The SSM2-targeting vector comprises LoxP-flanked Neomycin resistance gene (Neo) with 3′ polyadenylation signal (PolyA) and a 5′ Pgk promoter. This is followed by SYT-SSX2 cDNA and an encephalomyocarditis virus internal ribosomal entry site (IRES) fused to enhanced green fluorescent protein (EGFP) cDNA. This entire construct is flanked by a *ROSA26* homology region. A negative selection cassette comprising a Pgk promoter driving expression of diphtheria toxin A (DTA) was placed after the *ROSA* homology region. The SSM1 targeting vector has the same components except *IRES-EGFP*. Presence of Cre leads to recombination between the two LoxP sites, thereby removing the Neomycin gene along with its polyA, allowing transcription of SYT-SSX2 and *EGFP* from the endogenous *ROSA* promoter.

(B) The Myf5-targeting vector contains an encephalomyocarditis virus internal ribosomal entry site (IRES) fused to the Cre recombinase cDNA (Cre). This is followed by neomycin resistance gene (Neo) expressed by *MC1* promoter and flanked by two FRT sequences to allow removal of MC1-Neo by breeding to a flippase-expressing mouse if desired. This entire construct is flanked by sequences homologous to region of the Myf5 3′UTR. A thymidine kinase 1 (TK1)-negative-selection cassette was placed after the Myf5 homology region. This strategy enables transcription of a bicistronic *Myf5-IRES-Cre* RNA leading to expression of Cre recombinase without interfering with *Myf5* expression.

Myf5-Cre/SSM progenies were followed. About 8% of these mice were born significantly smaller than their siblings and usually died by 2 months of age. However, 100% of the surviving *Myf5-Cre/SSM* mice (18/18) developed tumors between the ages of 3–5 months, demonstrating complete penetrance in terms of tumor induction. Control littermates (>100) that included mice harboring only the *SSM* or *Myf5-Cre* alleles were followed for more than a year with no tumor induction or any other abnormalities. The *Myf5-Cre/SSM* mice that were born significantly smaller and died before 2 months did not harbor any apparent tumors and died of tumor-unrelated causes.

Multiple tumors (three to five per mouse) were detected within *Myf5-Cre/SSM* mice upon necropsy. Detection of very small tumors as well as potential metastasis was aided by expression of the EGFP marker protein incorporated in our design of SSM2 mice. All tumors detected within *Myf5-Cre/SSM2* mice had intense green fluorescence, characteristic of EGFP expression (Figures 2Bc and 2Be). Expression of SYT-SSX2 was also confirmed by RTPCR on total RNA from tumors (see Figure S2B in the Supplemental Data available with this article online). Most tumors were located within skeletal muscle, a predicted outcome since the fusion protein was induced within the skeletal-muscle-specific *Myf5* lineage (Table S1). However, a minority of small EGFP-positive tumors were observed in nonskeletal muscle tissue, such as the cerebellum (which is neither derived nor in close proximity to Myf5-derived tissue) suggestive of potential metastasis (Figure 2Bf).

Histological and Immunohistochemical Profiles of Mouse Tumors Recapitulate Human Synovial Sarcoma

On macroscopic examination, the mouse tumors were vascularized, often having a chalky white appearance distinct from the surrounding tissue (Figure 2Bb, arrows). Most frequently affected were the musculatures of the limb near joints and the intercostal region (Figures 2Ba, 2Bb, and 2Bd and Table S1). The tumors are often hemorrhagic (Figure 3Ac, green arrow), with cystic spaces often detected within larger tumors (Figure 3Ac, black arrow). Histology revealed striking similarity to human synovial sarcoma, with both biphasic (Figures 3Aa–3Ac) and monophasic variants (Figure 3Ad) identified. However, the monophasic variants greatly outnumbered biphasic (13 monophasic and 3 biphasic). This correlates well with data from human cases showing correlation of *SYT-SSX2*

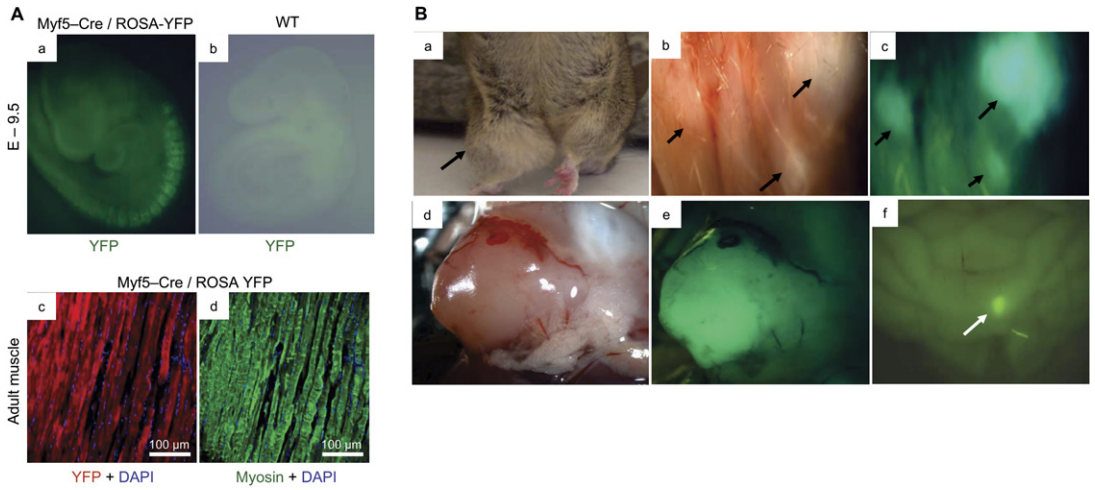

Figure 2. Tumor Induction within Myf5 Lineage

(A) E9.5 *Myf5-Cre/ROSA-YFP* embryos showing *Myf5* lineage in somites based on whole-mount fluorescence (Aa). Ab shows a wild-type littermate embryo. Adult *Myf5-Cre/ROSA-YFP* skeletal muscle sections demonstrate YFP expression ([Ac], red) within skeletal muscle fibers expressing skeletal-muscle-specific myosin ([Ad], green). Nuclei are marked blue by DAPI.

(B) Tumors within skeletal musculature of limbs (Ba and Bd) and intercostal region (Bb, arrows). Tumors are fluorescent due to EGFP expression ([Bc], arrows, and [Be]). Figure Bf shows a fluorescent potential metastatic lesion in brain.

with the monophasic subtype (Ladanyi et al., 2002). While smaller tumors were usually monophasic, often containing trapped skeletal muscle fibers (Figure 3Ad, black arrow), the larger tumors usually showed biphasic histology with epithelioid cells arranged in a glandular pattern amid spindle cells (Figure 3Ab, black arrow). Myxoid changes detected by alcian blue staining (Figure 3Ae) and fibrous changes detected by Masson's trichrome staining (Figure 3Af) also recapitulate features of human synovial sarcoma.

As mentioned elsewhere, synovial sarcomas coexpress epithelial as well as mesenchymal markers and often overexpress *Bcl-2*. This is faithfully recapitulated in tumors generated in our mouse model that show expression of epithelial cytokeratins (positive for cytokeratin AE1/AE2 cocktail and CAM5.2) as well as mesenchymal marker vimentin (Figures 3Ba–3Bd). In humans, synovial sarcoma is considered a high-grade tumor, which is recapitulated in our model based on widespread expression of the proliferation marker Mib (Figure 3Be). Since the tumors were induced within skeletal muscle lineage, immunohistochemistry for myogenin was done to rule out other muscle tumors, such as rhabdomyosarcomas, that are usually positive for myogenin (while synovial sarcomas are usually myogenin negative). The tumors generated in our model were negative for myogenin (Figure 3Bf). In summary, based on histopathology and immunohistochemistry, the mouse tumors strongly resemble human synovial sarcoma.

Transcriptional Profiles of the Mouse Tumors Recapitulate Human Synovial Sarcoma Profiles

To further compare the murine tumors to their human counterparts, transcriptional profiling analysis using Affymetrix mouse genome 430 2.0 gene chip was performed on five independent tumors and compared to four skeletal muscle samples from wild-type control mice. Hierarchical clustering of preprocessed and normalized expression profiles showed the expected segregation of tumors and normal muscle samples (Figure 4A). Subsequent significance analysis of microarrays (SAM) identified 1736 upregulated and 2341 downregulated genes at a false discovery rate (FDR) of <0.01 (Table S5). To determine if the expression profile of these mouse tumors simulated human synovial sarcoma, we compared our gene expression pattern to synovial sarcoma expression profiles present within several published human tumor expression data sets (Baird et al., 2005; Detwiller et al., 2005; Henderson et al., 2005; Nielsen et al., 2002). We first rank-ordered the genes in each data set according to their correlation to synovial sarcoma and extracted a list of significantly correlating genes as determined by permutation testing at a p value of <0.01 (Golub et al., 1999). The murine tumor data were similarly processed and converted to homologous human genes. The murine and human rank-ordered lists were compared via Spearman correlation testing. The results of the Spearman correlation showed small but significant similarities between murine SYT-SSX2-induced tumors and human synovial sarcomas (Table S2). This supported our hypothesis that the murine tumors are indeed synovial sarcomas.

We reasoned that the small correlations observed in the Spearman analysis were due to a previously unidentified SYT-SSX gene expression signature and that we could identify this signature by comparisons between the murine and human tumor data sets. To test this hypothesis, we employed a more sensitive statistical method, gene set enrichment analysis (GSEA). GSEA offers a straightforward means of measuring the "enrichment" of one gene

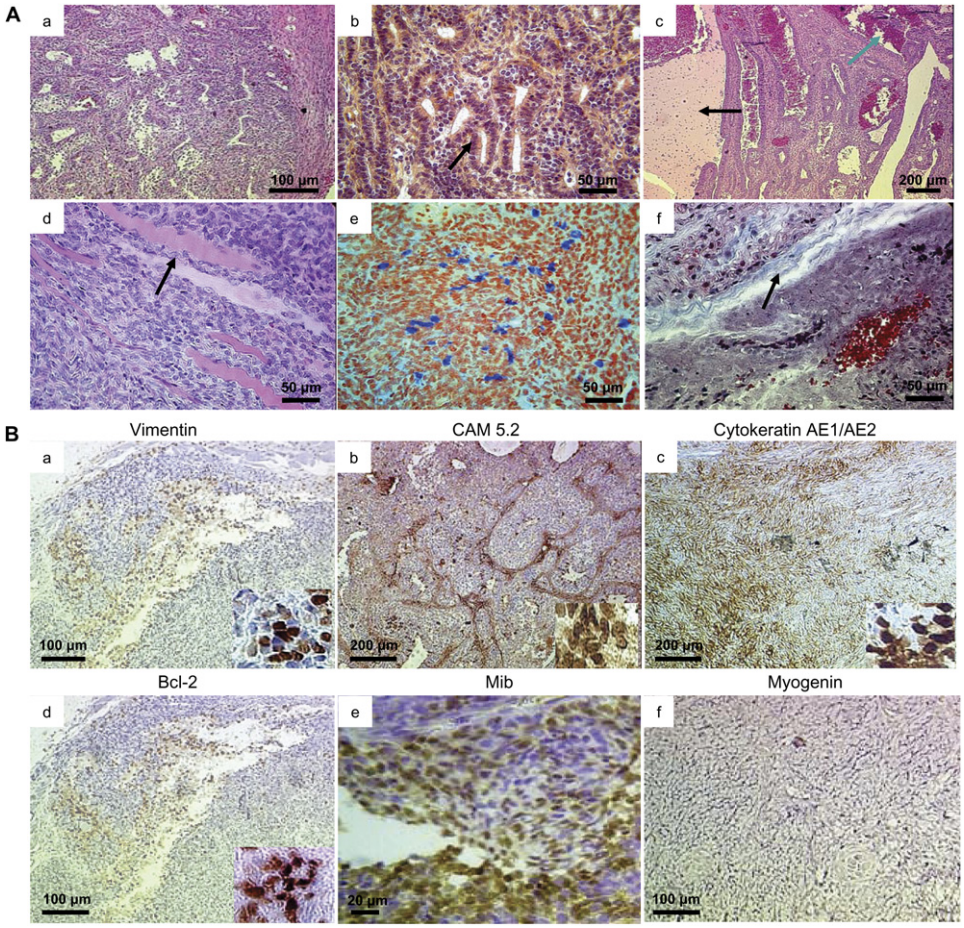

Figure 3. Tumor Histology and Immunohistochemistry

(A) Biphasic histology (Aa and Ab) showing epithelioid components arranged in a glandular pattern ([Ab], arrow). Biphasic tumor showing a cystic space ([Ac], black arrow) and hemorrhage ([Ac], green arrow). A monophasic tumor composed of spindle cells (Ad) showing trapped skeletal muscle fibers ([Ad], arrow). Tumors show myxoid change detected by alcian blue (Ae) and fibrosis detected by Masson's trichrome staining ([Af], black arrow). (B) Tumors are positive for vimentin (Ba), CAM 5.2 (Bb), Cytokeratin AE1/AE2 (Bc), and Bcl-2 (Bd). Tumors express proliferation marker Mib (Be) and are usually negative for myogenin (Bf).

set against an ordered data set in which genes are ranked according to their correlation to the phenotype of interest (Supplemental Data). GSEA has been used previously to compare data sets derived from different microarray platforms and from different species (Sweet-Cordero et al., 2005). We first derived an "SYT-SSX model gene set" from the murine tumor data and mapped the murine genes to their human counterparts. An initial GSEA comparison between this murine gene set and a human synovial sarcoma data set (Detwiller et al., 2005) did not demonstrate a statistically significant enrichment (ES 0.2, $p = 0.48$). This lack of enrichment does not necessarily indicate a strong dissimilarity between the murine model and the human disease but instead could be due to the mode of selection of the model signature or difficulties in comparing data sets across species or platforms. We therefore used this initial comparison as a "training set" to derive a common signature between the murine model and the Detwiller data set. We identified 55 genes that were enriched between the murine tumors and the training data set and named this list "SYT-SSX model synovial subset." Importantly, this gene set was largely distinct from a set of 249 synovial-sarcoma-specific genes derived from the Detwiller data set using SAM (only four genes overlapped between these two gene sets). To determine if this "SYT-SSX model synovial subset" of genes truly represented a new group of synovial sarcoma genes, we compared the performance of this gene set with the performance of a SAM-derived Detwiller synovial sarcoma gene set (designated as "human tumor synovial cell sarcoma gene set") using GSEA against three unique sarcoma "test data sets" (Baird, Nielsen, and Henderson data sets). The entire process is schematically represented in Figure 4B. The "SYT-SSX model synovial subset" is significantly represented in only human synovial sarcomas and not in other similar human sarcomas across all human tumor data sets (Table 1). This demonstrates that comparisons between the murine and human tumor data

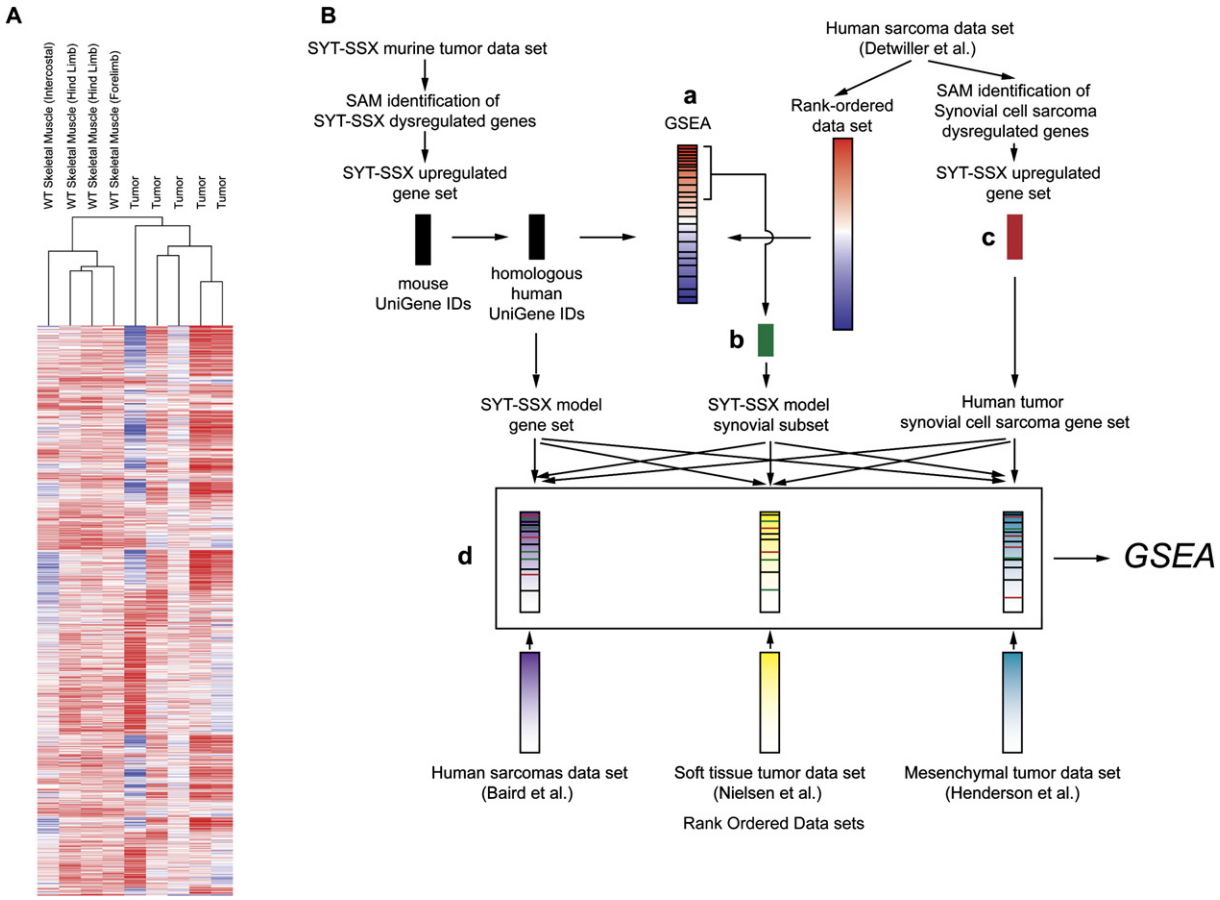

Figure 4. Microarray Analysis of Mouse Tumors

(A) Hierarchical clustering shows expected segregation of tumors and normal skeletal muscle.

(B) Strategy for gene set enrichment analyses. The initial GSEA is shown in (Ba). The SYT-SSX model synovial subset derived from this initial GSEA is represented in (Bb). The human synovial sarcoma control gene set is represented by (Bc). All three gene sets were compared in sequence to the phenotypes present in the remaining human tumor data sets (Bd).

sets can reveal synovial sarcoma-specific genes that could not otherwise be detected and further highlights the similarity between our murine tumors and human synovial sarcoma.

Myf5 Lineage Is a Potential Source of Synovial Sarcoma

In human synovial sarcomas, expression of SYT-SSX takes place from the endogenous *SYT* promoter, whereas in our model it takes place from the *ROSA* promoter within *Myf5* lineage. We therefore looked for expression of SYT within *Myf5* lineage as supporting evidence that *Myf5* lineage could be a bona fide source of this tumor. We bred the *Myf5-Cre* mice to *ROSA-YFP* reporter mice and looked for coexpression of YFP and SYT in embryos as well as in adult skeletal muscle of *Myf5-Cre*/*ROSA-YFP* progenies. We found that SYT is widely expressed within embryos that included almost all *YFP*-positive *Myf5* lineages (Figure 5A, left panel). Interestingly, SYT expression was also observed in a significant proportion of adult myonuclei (Figure 5A, right panel). To determine if SYT is expressed in muscle satellite cells, we did double immunostaining for *Pax7* and *SYT* that did not show any convincing expression of SYT within Pax7-expressing satellite cells (data not shown).

SYT-SSX2 Expression Restricts *Myf5* Lineage Expansion

Synovial-sarcoma-like tumors within *Myf5-Cre*/*SSM2* mice are intensely fluorescent due to expression of EGFP. Surprisingly, however, the surrounding skeletal muscle fibers are mostly GFP negative (Figure 5B). This observation could have a relatively trivial explanation, such as the *IRES* driving EGFP expression being inefficient within skeletal muscle as opposed to tumor cells. Alternatively, the explanation could be more biologically profound: the tumors are derived from Myf5-expressing cells, whereas the majority of the skeletal muscle in *Myf5-Cre*/SSM2 mice, though of normal appearance, is not derived from Myf5-expressing cells.

As part of an unrelated project, a conditional *Hox* gene was placed in the *ROSA* locus followed by the same

Table 1. GSEA of Gene Sets Upregulated in SYT-SSX and Synovial Cell Sarcoma Tumors Compared to Human Sarcoma Data Sets

	SYT-SSX Model Gene Set			SYT-SSX Model Synovial Subset			Human Tumor Synovial Cell Sarcoma Gene Set		
Human Cancer Phenotype Data Set	ES	NES	FWER p Value	ES	NES	FWER p Value	ES	NES	FWER p Value
Baird et al.									
Synovial cell sarcoma	0.167	0.780	0.791	0.582*	1.945*	0.001*	0.539*	2.030*	0.001*
Fibrosarcoma	−0.230	−1.084	0.379	0.352	1.184	0.364	−0.206	−0.749	0.713
Ewing's sarcoma	−0.160	−0.731	0.739	0.213	0.706	0.790	0.314	1.151	0.368
Osteosarcoma	−0.235	−1.102	0.345	−0.235	−0.782	0.708	−0.187	−0.672	0.765
Rhabdomyosarcoma	0.182	0.854	0.739	−0.254	−0.848	0.627	0.209	0.756	0.799
Leiomyosarcoma	0.241	1.123	0.415	−0.269	−0.911	0.587	−0.152	−0.558	0.799
Liposarcoma	0.201	0.932	0.609	−0.405	−1.365	0.155	−0.346	−1.285	0.224
Malignant fibrous histiosarcoma	−0.178	−0.831	0.668	−0.456	−1.572	0.048	−0.385	−1.424	0.116
Henderson et al.									
Monophasic synovial cell sarcoma	−0.293	−1.208	0.216	0.626*	1.565*	0.022*	0.712*	1.783*	<0.001*
Alveolar rhabdomyosarcoma	0.272	1.106	0.372	0.493	1.236	0.224	0.526	1.301	0.168
Ewing's sarcoma	0.276	1.127	0.342	0.476	1.185	0.266	0.327	0.818	0.702
Myxoid liposarcoma	−0.243	−0.989	0.470	0.418	1.060	0.439	−0.280	−0.699	0.764
Dedifferentiated chondrosarcoma	0.369	1.497	0.039	0.378	0.955	0.571	0.331	0.817	0.736
Embryonal rhabdomyosarcoma	0.236	0.974	0.524	0.358	0.927	0.584	0.603	1.501	0.042
Chondroblastoma	0.259	1.057	0.433	0.307	0.766	0.740	−0.393	−0.968	0.513
Fibromatosis	−0.253	−1.037	0.421	−0.303	−0.764	0.743	−0.354	−0.882	0.609
Well-differentiated liposarcoma	−0.242	−0.982	0.525	−0.327	−0.812	0.701	−0.535	−1.321	0.121
Lipoma	0.226	0.925	0.598	−0.330	−0.843	0.680	−0.572	−1.375	0.102
Osteosarcoma	0.325	1.316	0.142	−0.364	−0.903	0.623	−0.353	−0.874	0.651
Neurofibroma	−0.206	−0.837	0.697	−0.444	−1.113	0.349	−0.495	−1.226	0.230
Leiomyosarcoma	0.277	1.142	0.318	−0.504	−1.265	0.163	−0.379	−0.976	0.492
Chondrosarcoma	−0.237	−0.966	0.529	−0.511	−1.300	0.189	−0.442	−1.094	0.380
Chondromyxoid fibroma	−0.270	−1.093	0.379	−0.543	−1.392	0.098	−0.448	−1.104	0.360
Chordoma	−0.330	−1.344	0.132	−0.566	−1.372	0.107	−0.551	−1.369	0.111
Schwannoma	0.281	1.159	0.296	−0.598	−1.495	0.048	−0.555	−1.358	0.121
Nielsen et al.									
Synovial cell sarcoma	−0.293	−0.942	0.566	0.828*	1.568*	0.044*	0.679*	1.842*	0.001*
Malignant fibrous histiosarcoma	0.400	1.267	0.295	0.462	0.868	0.669	−0.511	−1.423	0.125
Gastrointestinal stromal tumor	−0.292	−0.962	0.517	0.444	0.817	0.695	−0.357	−0.985	0.498
Schwannoma	0.435	1.307	0.215	−0.437	−0.816	0.635	−0.394	−1.026	0.454
Leiomyosarcoma	0.244	0.793	0.648	−0.634	−1.152	0.406	−0.275	−0.753	0.785
Liposarcoma	−0.283	−0.916	0.600	−0.745	−1.376	0.166	−0.173	−0.480	0.807

Enrichment of genes upregulated in the mouse model and in human synovial sarcoma was analyzed by GSEA in human sarcoma data sets. The mouse model "synovial subset" comprises genes from the model set that show enrichment in an independent human sarcoma data set. Positive ES scores indicate enrichment in the cancer phenotype; negative ES scores indicate enrichment in the comparator class ("antienrichment"). Asterisks indicate statistical significance. As expected, the human synovial sarcoma gene set showed enrichment in human synovial sarcoma (positive ES score, significant FWER p value). Likewise, the mouse model "synovial subset" showed significant enrichment in human synovial sarcoma, while the full mouse model gene set showed nonsignificant enrichment. Neither the full mouse model gene set nor the synovial subset were significantly enriched in other human cancers. ES, enrichment score; NES, normalized enrichment score; FWER, family-wise error rate.

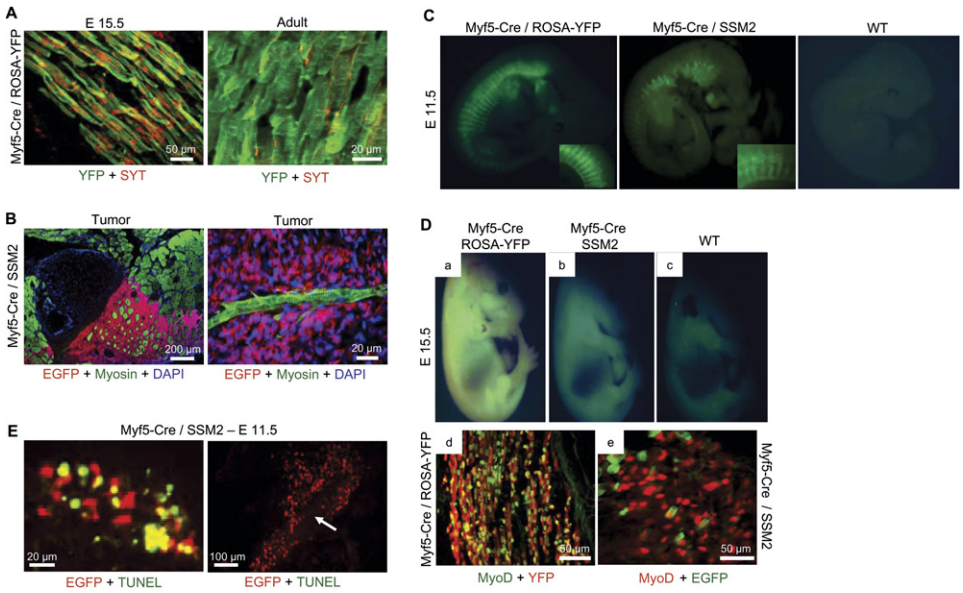

Figure 5. *SYT* Expression within Myf5 Lineage and Myf5 Lineage Restriction by SYT-SSX2

(A) SYT expression (red) is detected within YFP expressing *Myf5* lineage (green) in *Myf5*-Cre/*ROSA-YFP* E15.5 embryos (left panel) and adult skeletal muscle (right panel).

(B) A tumor arising near ribs (B, left panel and right panel) where all the tumor cells are expressing EGFP (red) while surrounding and trapped muscle fibers expressing myosin (green) are negative for EGFP. Nuclei are stained blue by DAPI.

(C) *Myf5* lineage in *Myf5-Cre/ROSA-YFP* E11.5 embryos (left panel) is marginally reduced in E11.5 *Myf5-Cre/SSM2* embryo (middle panel) based on whole-mount fluorescence. Insets show dermomyotomal regions at a higher magnification. Right panel shows wild-type littermate embryo.

(D) *Myf5* lineage is robust within *Myf5-Cre/ROSA-YFP* E15.5 embryos (Da) but undetectable in E15.5 *Myf5-Cre/SSM2* embryos (Db). Dc shows wild-type littermate embryo. This is also apparent by comparing sections through *Myf5-Cre/ROSA-YFP E15.5* embryos (Dd) to *Myf5-Cre/SSM2* E15.5 embryos (De). In (Dd), lineage marker YFP (red) colocalizes with skeletal-muscle-specific MyoD (green) compared to near absence of the lineage marker EGFP (green) in the presence of normal MyoD expression (red) in (De).

(E) Significant apoptosis (green nuclei) within somitic lineage of Myf5 expressing EGFP (red) in E11.5 *Myf5-Cre/SSM2* embryos (left panel). This is in contrast to absence of apoptosis (no green nuclei) within EGFP expressing Myf-5 lineage (red) near mesenchymal condensations of future ribs (right panel, white arrow) of the same embryo.

IRES-EGFP sequence used to construct the SSM2 mice. This mouse was bred to the *Myf5-Cre* mouse, and the skeletal muscle of the progeny showed readily detectable *IRES*-driven EGFP expression (data not shown). Therefore, lack of EGFP expression within skeletal muscle of *Myf5-Cre/SSM2* mice is not due to the *IRES* being inefficient in skeletal muscle, but rather is due to the absence or reduction of the *Myf5*-derived cell lineage in these mice. This implies that abrogating or severely restricting the *Myf5* lineage is compatible with normal development. In our laboratory we have generated a very efficient conditional cell ablation system in which an attenuated form of the *diphtheria toxin* gene (*DTA-176*) is targeted to the *ROSA* locus and dependent on Cre for its activation (Wu et al., 2006). This mouse was bred to the *Myf5-Cre* mouse, thereby killing all Myf5-expressing cells in the progeny containing both alleles. Remarkably, these pups are born with apparently normal musculature (Figure S2A).

Comparative analysis of *Myf5-Cre/SSM2* with *Myf5-Cre/ROSA-YFP* embryos was carried out to analyze *Myf5* lineage restriction by SYT-SSX2. This revealed that EGFP-mediated fluorescence within *Myf5-Cre/SSM2* embryos at E11.5 (Figure 5C, middle panel) was comparable to stage-matched *Myf5-Cre/ROSA-YFP* embryos (Figure 5C, left panel). However, *Myf5* lineage in *Myf5-Cre/SSM2* embryos is almost absent by E15.5 (Figure 5Db) when compared to stage-matched *Myf5-Cre/ROSA-YFP* embryos (Figure 5Da). This suggested that SYT-SSX2 expressing *Myf5* lineage is not viable. We next performed TUNEL assay on serial sections of *Myf5-Cre/SSM2* embryos at E11.5 (when *Myf5* lineage is still detectable) and found apoptosis within *Myf5* lineage (Figure 5E, left panel). An intriguing observation was that *Myf5* lineage near condensing mesenchyme of future rib cartilages does not show apoptosis (Figure 5E, right panel). This suggests that the microenvironment near cartilages may have survival factors preventing apoptosis by SYT-SSX2 that could partly explain the predilection of this tumor to arise near joints containing articular cartilages. Although the *Myf5* lineage is restricted by SYT-SSX2 expression, MyoD expression (marker for early skeletal muscle lineage) was normal within *Myf5-Cre/SSM2* E15.5 embryos, demonstrating that apoptosis within *Myf5* lineage does not compromise skeletal muscle genesis (Figures 5Dd and 5De).

Taken together, the above results suggest that SYT-SSX2 induces apoptosis within *Myf5* lineage and, only because Myf5-expressing cells are largely dispensable with respect to the formation of skeletal muscle, that

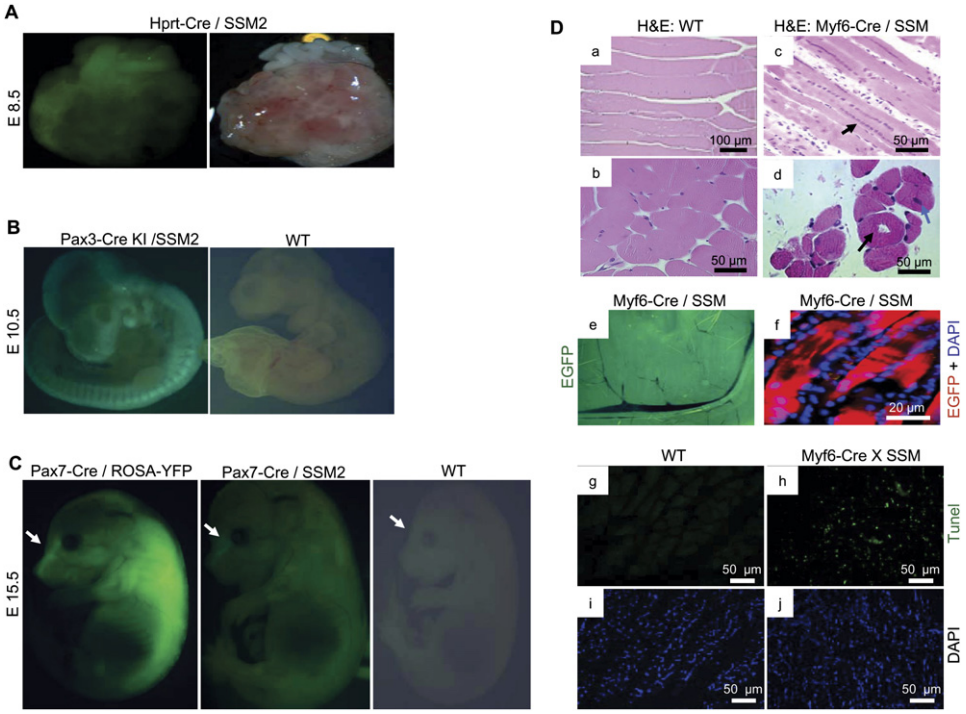

Figure 6. SYT-SSX2 Disrupts Normal Development

(A) Disorganized *Hprt-Cre/SSM2* fetal tissue (right panel) expressing EGFP (left panel).

(B) *Pax3* lineage within E10.5 *Pax3-Cre-KI/SSM2* embryo is detectable (left panel). Right panel shows wild-type (WT) littermate embryo.

(C) The left panel shows *Pax7* lineage within *Pax7-Cre/ROSA-YFP* E15.5 embryos, while the middle panel shows significantly reduced *Pax7* lineage within *Pax7-Cre/SSM2* embryo based on whole-mount fluorescence. The maxillary and nasal regions of *Pax7-Cre/SSM2* embryo show a larger proportion of surviving *Pax7* lineage compared to other regions (white arrows). Right panel shows wild-type (WT) littermate embryos.

(D) Myopathic skeletal muscle of *Myf6-Cre/SSM* adult mice show abnormal wavy fibers, myonuclear chain ([Dc], arrow), and significant variations in cross-sectional diameter between fibers ([Dd]) with occasional vacuolation ([Dd], black arrow) and central nuclei ([Dd], blue arrow). (Da) and (Db) show skeletal muscle sections from wild-type (WT) littermate. The myopathic skeletal muscle expresses EGFP detected in whole mount (De) and sections (Df). Apoptosis within myopathic muscles is detected by TUNEL assay ([Dh], green nuclei). (Dg) shows a TUNEL-negative control skeletal muscle section from wild-type (WT) littermate. (Di) and (Dj) correspond to the same field in (Dg) and (Dh) and show nuclei stained blue by DAPI.

Myf5-Cre/SSM mice have the opportunity to develop tumors at later times. Synovial sarcoma induction in our mouse model appears to be postnatal with a short latency period.

Early Embryonic Expression of SYT-SSX2 Induces Lethality

We next investigated whether SYT-SSX2 expression within any lineage, if induced early, could also generate synovial sarcoma. To investigate this, we bred our conditional SSM mice to *Hprt-Cre* mice that express Cre in very early-cleavage-stage embryos (Tang et al., 2002). No *Hprt-Cre/SSM* pups were ever recovered, indicating embryonic lethality. Although attempts to recover *Hprt-Cre/SSM* embryos failed, highly disorganized EGFP-expressing fetal tissue was detected at E8.5, indicating a dominant disruptive effect of SYT-SSX2 on normal embryonic development (Figure 6A).

We next investigated if SYT-SSX2 expression within skeletal muscle progenitors genetically upstream of *Myf5*, such as those expressing Pax3 and Pax7, leads to synovial sarcoma induction. We started by breeding the conditional *SSM* mice to *Pax3-Cre* knockin mice that express Cre recombinase from the endogenous *Pax3* locus (Engleka et al., 2005). *Pax3* is a transcription factor playing an important role in premigratory neural crest cells, as well as in early precursors of skeletal muscle (Epstein, 2000). No *Pax3-Cre/SSM* pups were obtained. However, embryos expressing EGFP in *Pax3* lineage pattern were recovered at E10.5 (Figure 6B) but not at E13.5, indicating that embryonic lethality occurred within this developmental time frame.

Next, the SSM mice were bred to mice expressing Cre from *Pax7* locus via an *IRES* placed in the 3′UTR of *Pax7* (Keller et al., 2004b). *Pax7* is a transcriptional factor that has important functions in skeletal muscle progenitors, particularly in the formation of muscle stem cells (satellite cells) that contribute to postnatal skeletal muscle formation and skeletal muscle regeneration (Jostes et al., 1990; Oustanina et al., 2004). Although no live progenies were obtained, *Pax7-Cre/SSM2* embryos were recovered at E15.5, indicating either late-embryonic or perinatal lethality (Figure 6C, middle panel).

Comparison of *Pax7-Cre/ROSA-YFP* (Figure 6C, left panel) and *Pax7-Cre/SSM2* (Figure 6C, middle panel)

embryos at E15.5 revealed significantly reduced *Pax7* lineage within *Pax7-Cre/SSM2* based on EGFP fluorescence. However, compared to other regions, a greater proportion of *Pax7* lineage was detected in the maxillary and nasal regions of *Pax7-Cre/SSM2* embryos (Figure 6C, arrows). This suggests that SYT-SSX2-expressing *Pax7* lineage is mostly not viable, except in proximity to the cartilaginous regions of developing maxilla and nasal turbinates. These observations are in good agreement with those made within *Myf5-Cre/SSM2* embryos.

Expression of SYT-SSX2 within Differentiated Cells of Skeletal Muscle Lineage Leads to Myopathy

We next investigated the effect of inducing SYT-SSX2 expression within more differentiated cells of skeletal muscle lineage. *Myf6* (*Mrf4*) is a myogenic regulatory factor expressed within myocytes and myofibers, a population more differentiated than and genetically downstream of Myf5-expressing myoblasts (Chanoine et al., 2004; Pownall et al., 2002). We have previously described the generation of mice expressing Cre from the *Myf6* locus via *IRES* (Keller et al., 2004a). These *Myf6-Cre* mice were bred to SSM mice. Although none of the resulting *Myf6-Cre/SSM* progenies developed tumors, all of them (8/8) developed myopathy and eventually died by 6 months of age. This was an unexpected observation since no human myopathy has been reported to be associated with SYT-SSX.

The myopathy within *Myf6-Cre/SSM* mice is characterized by abnormal wavy fibers and limited rhabdomyolysis (Figure 6Dc). Intrafiber vacuolation (Figure 6Dd, black arrow) and central nuclei (Figure 6Dd, blue arrow) further indicate skeletal muscle damage. Skeletal muscle regeneration was indicated by the presence of myonuclear chains (Figure 6Dc, arrow). These abnormal skeletal muscle fibers expressed EGFP, indicating expression of SYT-SSX2 (Figures 6De and 6Df). Significant apoptosis within these myopathic fibers was detected by TUNEL assay (Figure 6Dh), suggesting that SYT-SSX2 induces apoptosis within differentiated skeletal muscle fibers that leads to myopathy.

DISCUSSION

We report herein a mouse model of synovial sarcoma. This model recapitulates human synovial sarcoma based on clinical presentation, histology, immunohistochemical features, genetic signature (presence of SYT-SSX), and transcriptional profile. A targeted conditional strategy was adopted, enabling expression of the unique signature protein of synovial sarcoma, the SYT-SSX2 fusion protein, in chosen target cells. Tissue microenvironment is extremely important in tumorigenesis. Oncoproteins expressed in inappropriate microenvironments may not induce tumors or lead to biological effects unrelated to tumor formation. A conditional strategy circumvents such problems. A surprising outcome of our study is the identification of skeletal muscle lineage as a source of this tumor. Tumors were generated within *Myf5-Cre/SSM* mice with 100% penetrance, indicating that the fusion protein itself is sufficient to induce the chain of events leading to synovial sarcoma. In this context, it will be interesting to know whether continuous presence of SYT-SSX2 is required for tumor progression. We are currently investigating this possibility. It is also noteworthy that no tumors were detected by gross examination at necropsy within *Myf5-Cre/SSM* mice till after weaning (~3 weeks of age) indicating that, at least in our model, the transformation may occur after birth, with a relatively short latency period.

Tumors were generated within *Myf5* lineage, but not within the more differentiated *Myf6* lineage, thereby narrowing down the suspected cell of origin to myoblasts (Figure 7). Since we suspect tumor origin in our model to be postnatal, the best cellular candidate is Myf5-expressing myoblasts arising from activated satellite cells (muscle stem cells). However, quiescent satellite cells themselves, postnatally, could also be a potential source of synovial sarcoma. Satellite cells are marked by expression of Pax7. Expression of SYT-SSX2 within *Pax7* lineage induced embryonic lethality. However, this does not preclude Pax7-expressing cells from being a potential source of synovial sarcoma. In humans, the translocation is sporadic, and if it does occur within the *Pax7* compartment only some of these cells may harbor the translocation. However, by breeding *Pax7-Cre* mice with SSM mice, we expressed the fusion protein in virtually all Pax7-expressing cells and their lineage, thereby potentially overloading the system, causing lethality. Moreover, Pax7-expressing cells are not unique to the skeletal muscle lineage, as it also plays important roles in patterning of the dorsal neural tube during embryogenesis. However, after birth, *Pax7* expression is restricted to skeletal muscle satellite cells. To determine the possible role of the *Pax7* lineage as a source of synovial sarcoma in the context of skeletal muscle lineage, we are currently adopting the use of a CreER fusion protein instead of straight Cre recombinase. *Pax7-IRESCreER* allows modulation of the dosage and timing of Cre activation, by the requirement of the addition of the exogenous, small-molecule-inducing factor tamoxifen (Hayashi and McMahon, 2002). The presence of the SYT-SSX2 fusion protein in Pax7-expressing satellite cells could activate these quiescent cells and direct them toward a tumorigenic phenotype.

In human synovial sarcoma, SYT-SSX1 is associated with biphasic histology, while *SYT-SSX2* is associated with monophasic subtype (Ladanyi et al., 2002). This is recapitulated in our model, where we see a much higher frequency of monophasic tumors (13 monophasic versus 3 biphasic). An intriguing observation was a correlation between tumor size and tumor histology. While the smaller tumors showed monophasic histology, the larger tumors were biphasic. This seems to indicate that histology of the tumor may be a function of its "maturation" with more mature and advanced (hence larger) tumors associated with biphasic histology. The SYT-SSX1 type of fusion might be responsible for a faster rate of tumor "maturation" compared to SYT-SSX2 such that "maturation" is a reflection of mesenchymal-to-epithelial transition within

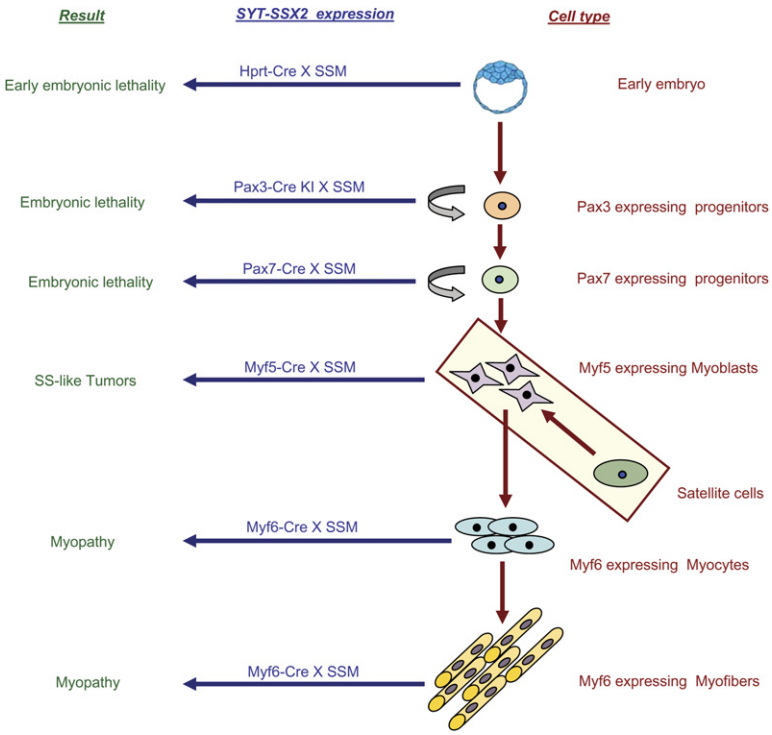

Figure 7. Summary of Breeding Experiments

Summary of results of expressing SYT-SSX2 fusion protein within various cells of skeletal muscle lineage. The yellow box highlights the suspected cell of origin: myoblasts arising from postnatal satellite cells.

the tumor, accounting for the statistical correlation of SYT-SSX1 to the biphasic subtype.

Synovial sarcoma in humans frequently arises near joints of limbs, a fact that is recapitulated in our model (Table S1). In *Myf5-Cre/SSM* embryos, we observed a greater proportion of surviving *Myf5* lineage near future rib cartilages, which were also the most frequent site of tumor induction in our model. This suggests a possible hypothesis that cartilaginous components may provide a particularly favorable niche for the survival of SYT-SSX2-expressing cells, thereby allowing their continued progression toward neoplasia, a potential explanation for occurrence of synovial sarcomas near joints that have cartilaginous articular regions.

Expression profiling of the synovial-sarcoma-like tumors in our mouse model revealed correlations between the murine model and human synovial sarcomas, establishing our model as a bona fide synovial sarcoma model. There are challenges in performing such comparisons, however. For example, while the human data sets compared synovial sarcomas to other tumors, our "SYT-SSX model" gene signature was obtained by comparing the murine tumors to normal mouse skeletal muscle because we lacked appropriate analogous murine tumors for such a comparison. Thus, our murine "SYT-SSX model gene set" likely represents both SYT-SSX dysregulated genes and genes that are dysregulated as a result of the transformation process. These "transformation" genes are likely to be dysregulated across many different sarcomas. This complicates comparisons between the human and murine tumors. We were able to extract a unique synovial sarcoma signature by comparing murine and human data sets. We then validated this signature by independently comparing it to human data sets not used in the initial screening process. This signature performed comparably to the human synovial signature in subsequent validation GSEAs and showed significant correlation between our synovial model and the human tumor profiles. This supports the notion that comparison of model systems to human tumors provides a unique opportunity to identify tumor-specific genes that could not be identified through comparative analysis of human tumors.

Disruption of normal embryogenesis by early ubiquitous expression of SYT-SSX2 underscores the dominant, disruptive effect of this protein on normal development, a potential explanation for the rarity of this tumor. The translocation itself might not be as rare an event as the disease itself. However, due to its strong disruptive effect, most embryos harboring this translocation early in development would be spontaneously aborted. This disruptive effect was also apparent within the more differentiated cells of skeletal muscle lineage, where myopathy was induced within musculature of *Myf6-Cre/SSM* mice. The myopathy was observed in the absence of tumor induction. However, it is possible that purposeful introduction of "second genetic hits" such as inactivation of *Trp53* or *Ink4a/ARF* in association with SYT-SSX2 might lead to the induction of synovial sarcoma in differentiated muscle. These "second genetic hits" may be required to initiate dedifferentiation of mature muscle, thereby facilitating tumor induction by SYT-SSX2, a possibility currently being tested.

Our laboratory has previously modeled alveolar rhabdomyosarcoma (ARMS) in mouse (Keller et al., 2004a). It is

informative to compare this model with the synovial sarcoma model. Both tumors appear to be induced by chromosomal translocations generating unique but separate fusion genes: *Pax3-Fkhr* or *Pax7-Fkhr* for ARMS and SYT-SSX1 or *SYT-SSX2* for synovial sarcoma. Both mouse models made use of a Cre/loxP-based conditional approach for expressing the respective fusion genes, although the specific strategies differed. The difference in strategy was dictated by differences in the expression patterns of the fusion gene. In ARMS, the expression pattern of PAX3-FKHR is controlled by the *cis*-regulatory elements associated with the *Pax3* locus, which has a specific expression domain in developing mouse embryo. To preserve this specific expression pattern, we chose to generate the fusion gene in response to Cre at the normal *Pax3* locus by juxtaposing the appropriate *Fkhr* genomic sequences to that locus (Keller et al., 2004a). In the absence of Cre, the *Pax3* locus retained normal *Pax3* function, while Cre-mediated recombination replaces *Pax3* with the *Pax3-Fkhr* fusion gene. In synovial sarcoma, the expression pattern of the *SYT-SSX* fusion gene is controlled by the *cis*-regulatory elements associated with the *SYT* locus, which has a widespread expression in developing mouse embryo. In this case, we could target the human *SYT-SSX2* fusion cDNA to the ubiquitously expressed *ROSA26* locus and use Cre to activate its expression in chosen tissues or cell types. Activation of either fusion protein, *Pax3-Fkhr* or SYT-SSX2, during early embryogenesis leads to embryonic lethality. However, while early expression of SYT-SSX2 in response to *Hprt-Cre* leads to very early lethality due to extensive disorganization of embryonic tissue, the midgestation lethality associated with expression of the *Pax3-Fkhr* fusion gene, on the other hand, is a partial phenocopy of *Pax3* deficiency, a consequence of this fusion protein turning off the normal *Pax3* locus (Keller et al., 2004b). The more extensive perturbations of development induced by SYT-SSX2 may reflect its more ubiquitous expression pattern and broader perturbations of transcription.

In the ARMS model, expressing Pax3-Fkhr within differentiating skeletal muscle lineage of *Myf6* induced tumors, albeit at very low penetrance (~1/200 mice). Cointroduction of conditional mutations in either *Trp53* or *INK4a/ARF* increased the penetrance to nearly 100%. In contrast, SYT-SSX2 expression within *Myf6* lineage induced myopathy without tumor induction, while expression within *Myf5* lineage induced synovial-sarcoma-like tumors with 100% penetrance. Therefore, either SYT-SSX2 has a stronger effect than *Pax3-Fkhr* in terms of respective tumor induction or in the synovial sarcoma model we targeted a population of cells that are more vulnerable to transformation by SYT-SSX2.

In summary, we report here the generation of a mouse model of synovial sarcoma based on a conditional, genetic strategy and demonstrate that Myf5-expressing myoblasts are a potential source of this tumor. This model should significantly aid our efforts in understanding the pathogenesis of this disease and serve as a useful preclinical platform to design and evaluate therapeutic modalities.

EXPERIMENTAL PROCEDURES

Targeted Mouse Line Production and Genotyping

Human SYT-SSX2 cDNA was obtained by RTPCR on total RNA from a synovial sarcoma tumor that was obtained as a deidentified patient sample through an approved University of Utah Institutional Review Board Protocol. This was used to generate targeting vectors as outlined in the Supplemental Data.

A clone consisting of an 8.4 kb segment of the *Myf5* region including the 3′UTR was isolated from a λ bacteriophage library of mouse strain SvJ-129 (Stratagene). This was used to generate the Myf5-Cre-targeting vector as outlined in the Supplemental Data.

Genotyping was carried out using PCR protocols and Southern blotting outlined in Figure S1 and the Supplemental Data. All studies involving animal subjects were approved by the University of Utah Institutional Animal Care and Use Committee and conducted strictly in accordance with the relevant protocol.

Histology and Immunohistochemistry

For histology, specimens were fixed overnight in 4% paraformaldehyde and embedded in paraffin wax following standard procedure. Four to eight micrometer sections were cut and mounted on slides for standard hematoxylin and eosin (H&E) staining, Masson's trichrome staining, or alcian blue staining.

Immunohistochemistry on 4 μm sections of paraffin-embedded samples was carried out by the ARUP laboratories at the University of Utah. Counterstaining was done with hematoxylin. For fluorescence-based detection, immunohistochemistry was performed on 8–12 μm frozen sections on samples fixed in 4% paraformaldehyde at 4°C for 3 hr. Please refer to the Supplemental Data for the list of primary and secondary antibodies used.

TUNEL Assay

TUNEL assay was performed using a fluorescein In Situ Cell Death Detection Kit (Roche) according to the manufacturer's instructions.

Microarray Analysis

RNA was extracted from tumors of female *Myf5-Cre/SSM* mice as well as from the skeletal muscle of wild-type age-matched female mice using TRIzol (Invitrogen) and purified using an RNeasy kit (Qiagen). A complete description of microarray analysis is provided in the Supplemental Data. The microarray data have been deposited in NCBI's Gene Expression Omnibus (GEO; http://www.ncbi.nlm.nih.gov/geo/) and are accessible through GEO Series accession number GSE6461.

Supplemental Data

The Supplemental Data include Supplemental Experimental Procedures, three supplemental figures, and seven supplemental tables and can be found with this article online at http://www.cancercell.org/cgi/content/full/11/4/375/DC1/.

ACKNOWLEDGMENTS

We thank Dr. R.L. Randall for providing RNA samples and Dr. Robert B. Weiss and Diane M. Dunn for assisting us with microarray analysis. M.H. was supported by the Terri Anna Perine Fund from the sarcoma services at Huntsman Cancer Institute at the University of Utah and the Bradley J. Breidinger Memorial Research award from the Sarcoma Foundation of America.

Received: October 18, 2006
Revised: December 2, 2006
Accepted: January 18, 2007
Published: April 9, 2007

REFERENCES

Baird, K., Davis, S., Antonescu, C.R., Harper, U.L., Walker, R.L., Chen, Y., Glatfelter, A.A., Duray, P.H., and Meltzer, P.S. (2005). Gene expression profiling of human sarcomas: Insights into sarcoma biology. Cancer Res. *65*, 9226–9235.

Chanoine, C., Della Gaspera, B., and Charbonnier, F. (2004). Myogenic regulatory factors: Redundant or specific functions? Lessons from Xenopus. Dev. Dyn. *231*, 662–670.

Clark, J., Rocques, P.J., Crew, A.J., Gill, S., Shipley, J., Chan, A.M., Gusterson, B.A., and Cooper, C.S. (1994). Identification of novel genes, SYT and SSX, involved in the t(X;18)(p11.2;q11.2) translocation found in human synovial sarcoma. Nat. Genet. *7*, 502–508.

Crew, A.J., Clark, J., Fisher, C., Gill, S., Grimer, R., Chand, A., Shipley, J., Gusterson, B.A., and Cooper, C.S. (1995). Fusion of SYT to two genes, SSX1 and SSX2, encoding proteins with homology to the Kruppel-associated box in human synovial sarcoma. EMBO J. *14*, 2333–2340.

de Bruijn, D.R., Baats, E., Zechner, U., de Leeuw, B., Balemans, M., Olde Weghuis, D., Hirning-Folz, U., and Geurts van Kessel, A.G. (1996). Isolation and characterization of the mouse homolog of SYT, a gene implicated in the development of human synovial sarcomas. Oncogene *13*, 643–648.

de Bruijn, D.R., Kater-Baats, E., Eleveld, M., Merkx, G., and Geurts Van Kessel, A. (2001). Mapping and characterization of the mouse and human SS18 genes, two human SS18-like genes and a mouse Ss18 pseudogene. Cytogenet. Cell Genet. *92*, 310–319.

de Leeuw, B., Suijkerbuijk, R.F., Olde Weghuis, D., Meloni, A.M., Stenman, G., Kindblom, L.G., Balemans, M., van den Berg, E., Molenaar, W.M., Sandberg, A.A., et al. (1994). Distinct Xp11.2 breakpoint regions in synovial sarcoma revealed by metaphase and interphase FISH: Relationship to histologic subtypes. Cancer Genet. Cytogenet. *73*, 89–94.

de Leeuw, B., Balemans, M., Olde Weghuis, D., and Geurts van Kessel, A. (1995). Identification of two alternative fusion genes, SYT-SSX1 and SYT-SSX2, in t(X;18)(p11.2;q11.2)-positive synovial sarcomas. Hum. Mol. Genet. *4*, 1097–1099.

Detwiller, K.Y., Fernando, N.T., Segal, N.H., Ryeom, S.W., D'Amore, P.A., and Yoon, S.S. (2005). Analysis of hypoxia-related gene expression in sarcomas and effect of hypoxia on RNA interference of vascular endothelial cell growth factor A. Cancer Res. *65*, 5881–5889.

dos Santos, N.R., de Bruijn, D.R., Kater-Baats, E., Otte, A.P., and van Kessel, A.G. (2000). Delineation of the protein domains responsible for SYT, SSX, and SYT-SSX nuclear localization. Exp. Cell Res. *256*, 192–202.

dos Santos, N.R., de Bruijn, D.R., and van Kessel, A.G. (2001). Molecular mechanisms underlying human synovial sarcoma development. Genes Chromosomes Cancer *30*, 1–14.

Engleka, K.A., Gitler, A.D., Zhang, M., Zhou, D.D., High, F.A., and Epstein, J.A. (2005). Insertion of Cre into the Pax3 locus creates a new allele of Splotch and identifies unexpected Pax3 derivatives. Dev. Biol. *280*, 396–406.

Epstein, J.A. (2000). Pax3 and vertebrate development. Methods Mol. Biol. *137*, 459–470.

Fisher, C. (1986). Synovial sarcoma: Ultrastructural and immunohistochemical features of epithelial differentiation in monophasic and biphasic tumors. Hum. Pathol. *17*, 996–1008.

Golub, T.R., Slonim, D.K., Tamayo, P., Huard, C., Gaasenbeek, M., Mesirov, J.P., Coller, H., Loh, M.L., Downing, J.R., Caligiuri, M.A., et al. (1999). Molecular classification of cancer: Class discovery and class prediction by gene expression monitoring. Science *286*, 531–537.

Guillou, L., Coindre, J., Gallagher, G., Terrier, P., Gebhard, S., de Saint Aubain Somerhausen, N., Michels, J., Jundt, G., Vince, D.R., Collin, F., et al. (2001). Detection of the synovial sarcoma translocation t(X;18) (SYT;SSX) in paraffin-embedded tissues using reverse transcriptase-polymerase chain reaction: A reliable and powerful diagnostic tool for pathologists. A molecular analysis of 221 mesenchymal tumors fixed in different fixatives. Hum. Pathol. *32*, 105–112.

Gure, A.O., Tureci, O., Sahin, U., Tsang, S., Scanlan, M.J., Jager, E., Knuth, A., Pfreundschuh, M., Old, L.J., and Chen, Y.T. (1997). SSX: A multigene family with several members transcribed in normal testis and human cancer. Int. J. Cancer *72*, 965–971.

Hayashi, S., and McMahon, A.P. (2002). Efficient recombination in diverse tissues by a tamoxifen-inducible form of Cre: A tool for temporally regulated gene activation/inactivation in the mouse. Dev. Biol. *244*, 305–318.

Henderson, S.R., Guiliano, D., Presneau, N., McLean, S., Frow, R., Vujovic, S., Anderson, J., Sebire, N., Whelan, J., Athanasou, N., et al. (2005). A molecular map of mesenchymal tumors. Genome Biol. *6*, R76.

Hibshoosh, H., and Lattes, R. (1997). Immunohistochemical and molecular genetic approaches to soft tissue tumor diagnosis: A primer. Semin. Oncol. *24*, 515–525.

Hiraga, H., Nojima, T., Abe, S., Sawa, H., Yamashiro, K., Yamawaki, S., Kaneda, K., and Nagashima, K. (1998). Diagnosis of synovial sarcoma with the reverse transcriptase-polymerase chain reaction: Analyses of 84 soft tissue and bone tumors. Diagn. Mol. Pathol. *7*, 102–110.

Jackson, R.J., Howell, M.T., and Kaminski, A. (1990). The novel mechanism of initiation of picornavirus RNA translation. Trends Biochem. Sci. *15*, 477–483.

Jang, S.K., and Wimmer, E. (1990). Cap-independent translation of encephalomyocarditis virus RNA: Structural elements of the internal ribosomal entry site and involvement of a cellular 57-kD RNA-binding protein. Genes Dev. *4*, 1560–1572.

Jostes, B., Walther, C., and Gruss, P. (1990). The murine paired box gene, Pax7, is expressed specifically during the development of the nervous and muscular system. Mech. Dev. *33*, 27–37.

Kawai, A., Woodruff, J., Healey, J.H., Brennan, M.F., Antonescu, C.R., and Ladanyi, M. (1998). SYT-SSX gene fusion as a determinant of morphology and prognosis in synovial sarcoma. N. Engl. J. Med. *338*, 153–160.

Keller, C., Arenkiel, B.R., Coffin, C.M., El-Bardeesy, N., DePinho, R.A., and Capecchi, M.R. (2004a). Alveolar rhabdomyosarcomas in conditional Pax3:Fkhr mice: Cooperativity of Ink4a/ARF and Trp53 loss of function. Genes Dev. *18*, 2614–2626.

Keller, C., Hansen, M.S., Coffin, C.M., and Capecchi, M.R. (2004b). Pax3:Fkhr interferes with embryonic Pax3 and Pax7 function: Implications for alveolar rhabdomyosarcoma cell of origin. Genes Dev. *18*, 2608–2613.

Ladanyi, M., and Bridge, J.A. (2000). Contribution of molecular genetic data to the classification of sarcomas. Hum. Pathol. *31*, 532–538.

Ladanyi, M., Antonescu, C.R., Leung, D.H., Woodruff, J.M., Kawai, A., Healey, J.H., Brennan, M.F., Bridge, J.A., Neff, J.R., Barr, F.G., et al. (2002). Impact of SYT-SSX fusion type on the clinical behavior of synovial sarcoma: A multi-institutional retrospective study of 243 patients. Cancer Res. *62*, 135–140.

Lim, F.L., Soulez, M., Koczan, D., Thiesen, H.J., and Knight, J.C. (1998). A KRAB-related domain and a novel transcription repression domain in proteins encoded by SSX genes that are disrupted in human sarcomas. Oncogene *17*, 2013–2018.

Limon, J., Dal Cin, P., and Sandberg, A.A. (1986). Translocations involving the X chromosome in solid tumors: Presentation of two sarcomas with t(X;18)(q13;p11). Cancer Genet. Cytogenet. *23*, 87–91.

Nagai, M., Tanaka, S., Tsuda, M., Endo, S., Kato, H., Sonobe, H., Minami, A., Hiraga, H., Nishihara, H., Sawa, H., and Nagashima, K. (2001). Analysis of transforming activity of human synovial sarcoma-associated chimeric protein SYT-SSX1 bound to chromatin remodeling factor hBRM/hSNF2 alpha. Proc. Natl. Acad. Sci. USA *98*, 3843–3848.

Nielsen, T.O., West, R.B., Linn, S.C., Alter, O., Knowling, M.A., O'Connell, J.X., Zhu, S., Fero, M., Sherlock, G., Pollack, J.R., et al. (2002). Molecular characterisation of soft tissue tumours: A gene expression study. Lancet *359*, 1301–1307.

Oustanina, S., Hause, G., and Braun, T. (2004). Pax7 directs postnatal renewal and propagation of myogenic satellite cells but not their specification. EMBO J. *23*, 3430–3439.

Panagopoulos, I., Mertens, F., Isaksson, M., Limon, J., Gustafson, P., Skytting, B., Akerman, M., Sciot, R., Dal Cin, P., Samson, I., et al. (2001). Clinical impact of molecular and cytogenetic findings in synovial sarcoma. Genes Chromosomes Cancer *31*, 362–372.

Pelmus, M., Guillou, L., Hostein, I., Sierankowski, G., Lussan, C., and Coindre, J.M. (2002). Monophasic fibrous and poorly differentiated synovial sarcoma: Immunohistochemical reassessment of 60 t(X;18)(SYT-SSX)-positive cases. Am. J. Surg. Pathol. *26*, 1434–1440.

Perani, M., Ingram, C.J., Cooper, C.S., Garrett, M.D., and Goodwin, G.H. (2003). Conserved SNH domain of the proto-oncoprotein SYT interacts with components of the human chromatin remodelling complexes, while the QPGY repeat domain forms homo-oligomers. Oncogene *22*, 8156–8167.

Poteat, H.T., Corson, J.M., and Fletcher, J.A. (1995). Detection of chromosome 18 rearrangement in synovial sarcoma by fluorescence in situ hybridization. Cancer Genet. Cytogenet. *84*, 76–81.

Pownall, M.E., Gustafsson, M.K., and Emerson, C.P., Jr. (2002). Myogenic regulatory factors and the specification of muscle progenitors in vertebrate embryos. Annu. Rev. Cell Dev. Biol. *18*, 747–783.

Renwick, P.J., Reeves, B.R., Dal Cin, P., Fletcher, C.D., Kempski, H., Sciot, R., Kazmierczak, B., Jani, K., Sonobe, H., and Knight, J.C. (1995). Two categories of synovial sarcoma defined by divergent chromosome translocation breakpoints in Xp11.2, with implications for the histologic sub-classification of synovial sarcoma. Cytogenet. Cell Genet. *70*, 58–63.

Skytting, B., Nilsson, G., Brodin, B., Xie, Y., Lundeberg, J., Uhlen, M., and Larsson, O. (1999). A novel fusion gene, SYT-SSX4, in synovial sarcoma. J. Natl. Cancer Inst. *91*, 974–975.

Smith, S., Reeves, B.R., Wong, L., and Fisher, C. (1987). A consistent chromosome translocation in synovial sarcoma. Cancer Genet. Cytogenet. *26*, 179–180.

Smith, M.E., Fisher, C., Wilkinson, L.S., and Edwards, J.C. (1995). Synovial sarcoma lack synovial differentiation. Histopathology *26*, 279–281.

Soriano, P. (1999). Generalized lacZ expression with the ROSA26 Cre reporter strain. Nat. Genet. *21*, 70–71.

Srinivas, S., Watanabe, T., Lin, C.S., William, C.M., Tanabe, Y., Jessell, T.M., and Costantini, F. (2001). Cre reporter strains produced by targeted insertion of EYFP and ECFP into the ROSA26 locus. BMC Dev. Biol. *1*, 4.

Sweet-Cordero, A., Mukherjee, S., Subramanian, A., You, H., Roix, J.J., Ladd-Acosta, C., Mesirov, J., Golub, T.R., and Jacks, T. (2005). An oncogenic KRAS2 expression signature identified by cross-species gene-expression analysis. Nat. Genet. *37*, 48–55.

Tang, S.H., Silva, F.J., Tsark, W.M., and Mann, J.R. (2002). A Cre/loxP-deleter transgenic line in mouse strain 129S1/SvImJ. Genesis *32*, 199–202.

Thaete, C., Brett, D., Monaghan, P., Whitehouse, S., Rennie, G., Rayner, E., Cooper, C.S., and Goodwin, G. (1999). Functional domains of the SYT and SYT-SSX synovial sarcoma translocation proteins and co-localization with the SNF protein BRM in the nucleus. Hum. Mol. Genet. *8*, 585–591.

Weiss, S.W., and Goldblum, J.R. (2001). Enzinger and Weiss's Soft Tissue Tumors, Fourth Edition (St. Louis, MO: Mosby, Inc.).

Willeke, F., Mechtersheimer, G., Schwarzbach, M., Weitz, J., Zimmer, D., Lehnert, T., Herfarth, C., von Knebel Doeberitz, M., and Ridder, R. (1998). Detection of SYT-SSX1/2 fusion transcripts by reverse transcriptase-polymerase chain reaction (RT-PCR) is a valuable diagnostic tool in synovial sarcoma. Eur. J. Cancer *34*, 2087–2093.

Wu, S., Wu, Y., and Capecchi, M.R. (2006). Motoneurons and oligodendrocytes are sequentially generated from neural stem cells but do not appear to share common lineage-restricted progenitors in vivo. Development *133*, 581–590.

Zambrowicz, B.P., Imamoto, A., Fiering, S., Herzenberg, L.A., Kerr, W.G., and Soriano, P. (1997). Disruption of overlapping transcripts in the ROSA beta geo 26 gene trap strain leads to widespread expression of beta-galactosidase in mouse embryos and hematopoietic cells. Proc. Natl. Acad. Sci. USA *94*, 3789–3794.

Accession Numbers

The microarray data have been deposited in NCBI's Gene Expression Omnibus (GEO; http://www.ncbi.nlm.nih.gov/geo/) and are accessible through GEO Series accession number GSE6461.